KI REPORTS
KIReports.org

Raman Spectroscopy for the Diagnosis of Intratubular Triamterene Crystallization

C. John Sperati[1], Chi Zhang[2], Marco Delsante[3], Rajib Gupta[4], Serena Bagnasco[3] and Ishan Barman[2,5]

[1]Division of Nephrology, Johns Hopkins University School of Medicine, Baltimore, Maryland, USA; [2]Department of Mechanical Engineering, Johns Hopkins University, Baltimore, Maryland, USA; [3]Department of Pathology, Johns Hopkins University School of Medicine, Baltimore, Maryland, USA; [4]Department of Laboratory Medicine and Pathology, University of Minnesota, Minneapolis, Minnesota, USA; and [5]Department of Oncology, Johns Hopkins University School of Medicine, Baltimore, Maryland, USA

Correspondence: C. John Sperati, Division of Nephrology, Johns Hopkins University School of Medicine, 1830 E Monument Street, Room 416, Baltimore, Maryland 21287, USA. E-mail: jsperati@jhmi.edu

Kidney Int Rep (2018) **3,** 997–1003; https://doi.org/10.1016/j.ekir.2018.03.010

INTRODUCTION

Medication-induced crystalluria is a well-recognized phenomenon and can result in nephrolithiasis and/or acute kidney injury (AKI). Common etiologies such as indinavir, acyclovir, and sulfadiazine, produce characteristic crystals easily identified on microscopic evaluation of the urine.[1,2] A known, but less commonly considered, agent is triamterene. A potassium-sparing diuretic typically combined with a thiazide in the management of hypertension, triamterene-hydrochlorothiazide prescriptions totaled 10,970,464 in 2014.[3] Triamterene crystals, however, are often not appreciated on urine microscopy, and histologically these crystals can be confused with calcium oxalate or 2,8-dihydroxyadenine (2,8-DHA). Herein is presented a case of AKI associated with intratubular triamterene crystallization confirmed by Raman spectroscopy.

Kidney biopsy remains the gold standard for definitive diagnosis of most etiologies of kidney disease. A diagnosis is rendered largely from visual pattern recognition, and this is limited by pathologist experience and the ability of current techniques to adequately distinguish pathologic findings. Novel imaging methods are being applied to kidney biopsy material that do not rely on operator recall, thereby permitting definitive diagnosis of challenging material.[4] Raman spectroscopy is one such technique, which relies on intrinsic vibrational signatures to perform label-free molecular fingerprinting.[5] Spontaneous Raman spectroscopy measures the inelastic scattering of light following the interaction of monochromatic radiation with a sample, permitting noninvasive, nondestructive analysis without the use of exogenous labels (Figure 1). Raman spectroscopy of kidney tissue chemistry and its utility for diagnosis remain largely unexplored.

CASE PRESENTATION AND METHODS

Case Presentation

A 51-year-old woman was hospitalized for AKI in the setting of cellulitis. Her history was notable for Stage 3 chronic kidney disease (serum creatinine 1.8 mg/dl; estimated glomerular filtration rate 37 ml/min per 1.73 m^2), hypertension, and psoriasis. She had been prescribed furosemide and triamterene-hydrochlorothiazide for hypertension, and she had experienced several prior episodes of AKI attributed to pre-renal azotemia. She had no history of nephrolithiasis, and family history was remarkable for a sister with end-stage renal disease (ESRD). At presentation, serum creatinine was 3.2 mg/dl, urine protein 119 mg per day, and urinalysis revealed 23 white blood cells per high-power field without hematuria or cellular casts (Table 1). Ultrasound demonstrated the right kidney to be 8.5 cm and left 9.2 cm, both with normal echogenicity. With antibiotics and discontinuation of diuretics, creatinine returned to baseline. She underwent kidney biopsy for further evaluation of her chronic kidney disease given the family history of ESRD.

On biopsy, 31 glomeruli were present, of which 2 were globally sclerosed. Moderate tubular injury was present with sparse interstitial inflammatory infiltrate and less than 10% interstitial fibrosis. Mildly dilated tubules contained radially arranged rod- or rhomboid-shaped crystals that filled the tubular lumen in most places, at times associated with giant cell reaction

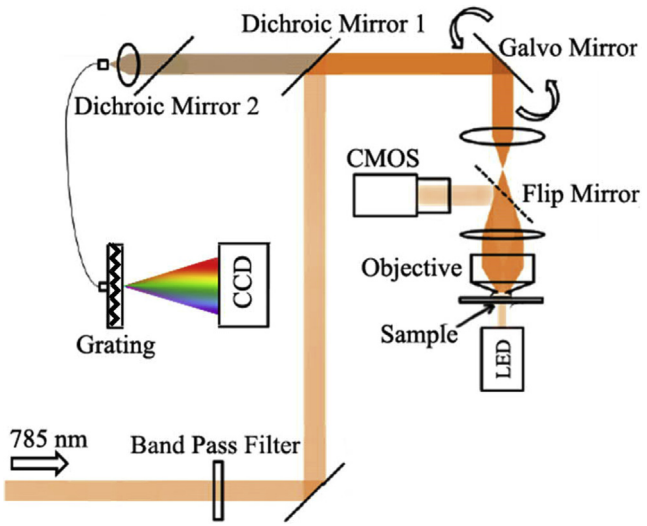

Figure 1. Raman spectroscopy microscope. The excitation source was a compact holographic grating-stabilized 785-nm laser diode. Dichroic mirror 1 redirected the collimated beam through the dual-axes galvanometer mirrors. A ×60 oil-immersion objective lens focused the laser beam and collected the backscattered light from the sample. Raman signals retraced the excitation beam path and passed through dichroic mirror 1. The Raman signal was delivered to the imaging spectrograph, whose spectral output was captured by a thermoelectrically cooled charge-coupled device (CCD). A light-emitting diode (LED) was used as an illuminating source and coupled with a complementary metal-oxide-semiconductor (CMOS) camera to identify morphological features of the sample in the same field of view. A flip mirror allowed switching between the Raman signal acquisition and bright field imaging.

(Figure 2a–e). The crystals were yellow-brown on hematoxylin-eosin and periodic acid-Schiff stain, black/gray on methenamine silver, pale blue on Masson trichrome stain, and were polarizable with Maltese cross formation. In comparison, 2,8-DHA crystals are similar in color and shape to triamterene and are also birefringent. Oxalate, however, is usually clear to blue and does not form Maltese crosses.

Table 1. Laboratory values

Test	Admission	2 mo before admission
Blood urea nitrogen, mg/dl	28	32
Creatinine, mg/dl	3.2	1.8
Albumin, g/dl	3.1	3.8
Urinalysis		
Specific gravity	1.012	1.012
pH	6.5	6.5
Protein	Trace	Negative
Hemoglobin	Negative	Negative
Nitrite	Negative	Negative
Leukocyte esterase	Moderate	Moderate
White blood cells, hpf	23	3
Red blood cells, hpf	0	0
Epithelial cells, hpf	1	0
24-hour urine, mg	119	–

hpf, high-power field.

Given the remarkable visual similarity to 2,8-DHA crystals seen in adenine phosphoribosyltransferase (APRT) deficiency, *APRT* was sequenced and enzymatic activity was measured. No sequence variants were detected, and enzymatic activity was within normal limits. Given the family history of ESRD, definitive identification of the crystals to exclude APRT deficiency was made by Raman spectroscopy.

Control regions (Figure 3a) and 3 separate biopsy sites containing crystals (Figure 3b) were probed. The spectral similarity between the tissue crystal and that of a pure triamterene sample is evident visibly and statistically ($R = 0.75$; Figure 3c). Figure 3d shows the spectral overlay from the tissue crystals and a pure 2,8-DHA sample ($R = 0.11$). Additionally, the correlation coefficients of a pure sample of triamterene with 2,8-DHA and calcium oxalate monohydrate were 0.09 and −0.06, respectively.

At 2-year follow-up, creatinine was 1.2 mg/dl (estimated glomerular filtration rate 57 ml/min per 1.73 m^2) off triamterene-hydrochlorothiazide.

Methods

Five-micrometer sections of optimal cutting temperature embedded frozen tissue, triamterene (Sigma-Aldrich, St. Louis, MO), and 2,8-DHA (Toronto Research Chemicals, Toronto, Ontario, Canada) were placed separately on quartz coverslips. For Raman measurements, an inverted confocal Raman microscope was adapted from a published design.[6] The excitation source was a compact LM series volume holographic grating-stabilized laser diode ($\lambda_{em} = 785$ nm) (Ondax, Monrovia, CA) with a clean-up filter (LL01-785-12.5; Semrock, Rochester, NY). The laser was redirected to the dual-axes galvanometer mirrors (GVS112; Thorlabs, Newton, NJ) via a dichroic laser-flat beam splitter (LPD01-785RU-25; Semrock). The galvanometer mirrors enable high-speed lateral scanning in the sample plane. A ×60 oil-immersion objective lens focused the laser and collected backscattered light from the sample. The Raman scattering light was collected by a 50-mm multimode fiber (M14L01; Thorlabs), delivered to a HoloSpec f/1.8 spectrograph (Kaiser Optical Systems, Ann Arbor, MI), and finally detected by an iDus charge-coupled device camera (DU420A-BEX2-DD; Andor, Belfast, UK). Exposure time was 10 seconds at 5-mW laser power. Cosmic ray and fluorescence signals were removed before spectral analysis. Customized LabView 2013 (National Instruments, Austin, TX) and MATLAB 2013 (Mathworks, Natick, MA) modules were used for system control and data analysis. Spectra were compared by Pearson correlation coefficient.

Coding regions and introns within 20 base pairs of the exon/intron boundaries of *APRT* (NM_000485.2)

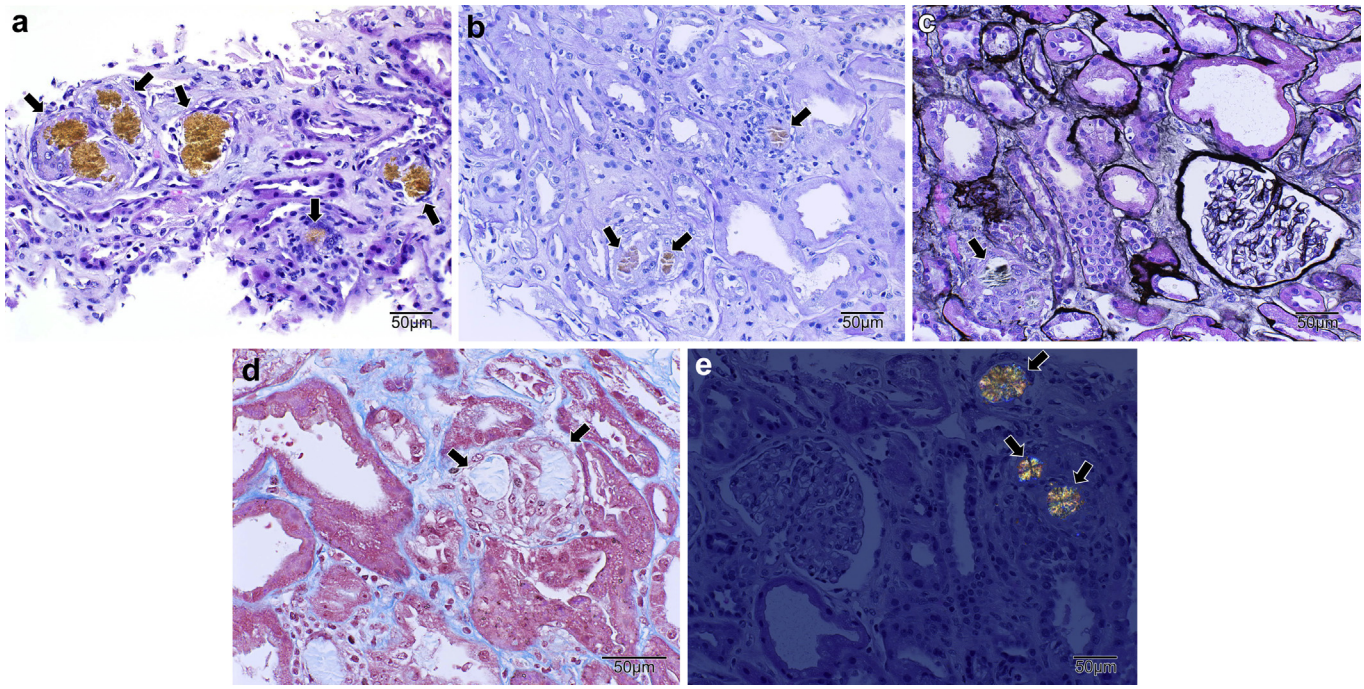

Figure 2. Intratubular triamterene crystals (arrows). (a) Brownish-yellow with associated giant cell reaction by hematoxylin-eosin, original magnification ×100; (b) brownish-yellow by periodic acid–Schiff, original magnification ×100; (c) black/gray by methenamine silver, original magnification ×100; (d) pale blue by Masson trichrome, original magnification ×160; and (e) Birefringence and Maltese cross formation under polarized light, original magnification ×100.

were amplified and sequenced in the forward and reverse directions using automated fluorescent dideoxy sequencing methods (Baylor Miraca Genetics Laboratory, Houston, TX). Semi-quantitative assay of APRT enzymatic activity in dried blood spots was performed by UCSD Biochemical Genetics Laboratory (San Diego, CA).

DISCUSSION

Combination triamterene-hydrochlorothiazide was the number 1 prescribed medication in the United States in 1986, and as of 2014 was number 75.[3] Renal excretion represents the major route of elimination, with urinary crystals present in 50% to 100% of individuals taking the drug.[7,8] Triamterene nephrolithiasis was first reported in 1979 with an incidence of 1:1500 to 1:2500.[9,10] Although crystalluria and nephrolithiasis are not rare, triamterene-associated AKI has been reported only on occasion.

Triamterene can crystallize in the renal tubules of rats.[8] In 1986, polarizable crystals primarily within the cytoplasm of distal tubular epithelial cells were noted in a patient following a triamterene-hydrochlorothiazide overdose associated with AKI.[11] This was followed by a case of irreversible AKI in which yellowish, polarizable crystals were found to obstruct the tubular lumen in association with multinucleated giant cells.[12] Our patient's kidney function slowly improved with discontinuation of triamterene, leading one to speculate that the removal of precipitated triamterene from the renal tubules may occur over time. It was not until 2014 when another 2 cases of triamterene-associated AKI were reported, one of which was originally misdiagnosed as 2,8-DHA crystal deposition due to APRT deficiency.[13]

Our crystals were yellow-brown, polarizable with Maltese cross formation, and had accompanying giant cell reaction, as has been reported for triamterene. In comparison, 2,8-DHA crystals are also birefringent, can be similar in color and shape to triamterene, and may form Maltese crosses in urine but not typically in renal parenchyma.[14,15] Calcium oxalate crystals are birefringent, but are usually clear to blue and do not form Maltese crosses.

APRT deficiency (OMIM #102600) is an autosomal recessive disorder resulting in metabolism of adenine to 2,8-DHA. Patients are at increased risk for AKI, chronic kidney disease is present in approximately one-third of patients, and 10% may reach ESRD. Nephrolithiasis is common in APRT deficiency, and the stones are radiolucent.[14,16] A diagnosis of APRT deficiency was not supported by either genetic or biochemical analysis. Given, however, the visual similarity to 2,8-DHA crystals and the family history of ESRD, APRT deficiency was definitively excluded by positively

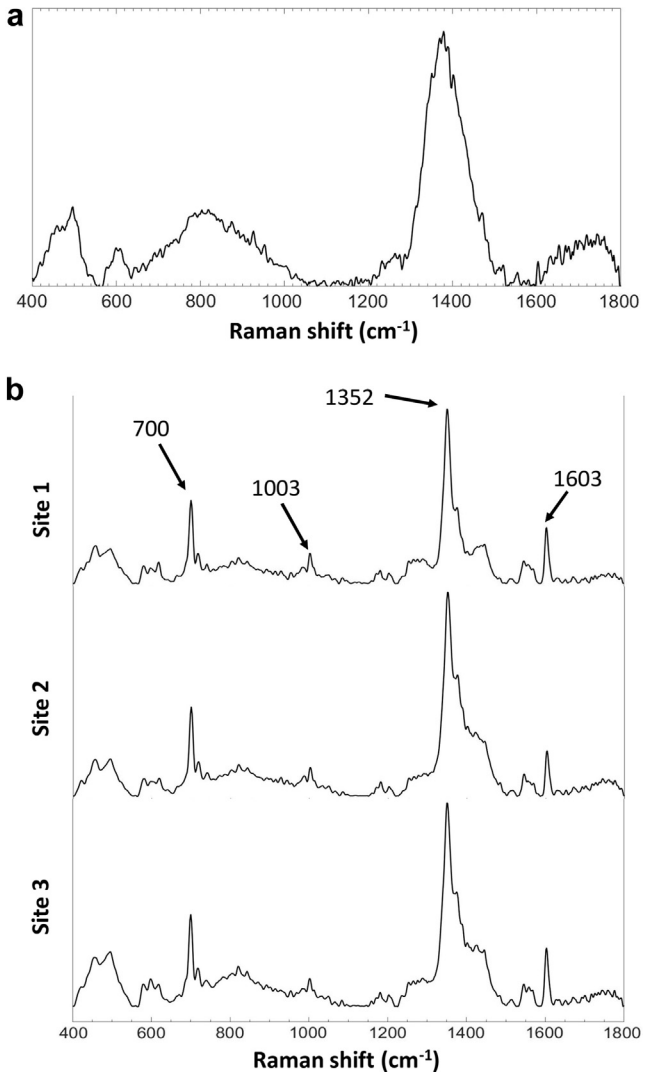

Figure 3. (a) Raman spectrum from tissue without crystals. (b) Raman spectra of intratubular triamterene crystals from 3 sites. The presence of prominent peaks at 700, 1003, 1352, and 1603 cm^{-1}, and their relative peak intensities, were closely mirrored at all 3 crystal sites. (Continued)

identifying the crystals as triamterene by Raman spectroscopy.

The characterization of urinary calculi is commonplace, but limited work has been done to identify crystal species in kidney tissue.[17–19] Raman spectroscopy has been used to identify oxalate in tissue from patients with known oxalosis, as well as calcium crystals in kidney tumors.[20,21] Several groups have used Fourier-transformed infrared spectroscopy to confirm 2,8-DHA, as well as other crystals in kidney biopsies.[15,22,23] Our case extends the application of Raman spectroscopy to making a *de novo* clinical diagnosis from the analysis of unidentified crystalline material. These results underscore the molecular specificity of Raman spectroscopy and its ability to identify crystals in a biopsy specimen. As databases of acquired spectra grow, Raman spectroscopy could be used in the characterization of other biopsy findings, such as unidentified pigmented material, constitution of tubular casts, cellular infiltrates, and drug-induced kidney injury.

To this end, investigators have used Raman spectroscopy to identify hydroxyethyl starch in osmotic lesions from patients with AKI after exposure to the agent.[24] The presence of hydroxyethyl starch in kidney allografts taken from hydroxyethyl starch–resuscitated donors also has been correlated with graft outcome.[25] In a mouse model of anti-glomerular basement membrane disease, Raman spectroscopy was able to distinguish the severity of glomerulonephritis with 98% accuracy by using principal component and linear discriminant analysis.[26] An automated measurement of tissue injury can add significantly to the pathological information derived from an experienced pathologist. Furthermore, Raman spectroscopy has shown promise in prognosticating renal allograft outcome from the urine of deceased donors.[27] Using silver nanoparticles for surface-enhanced Raman spectroscopy of deceased donor urine, Chi *et al.*[27] achieved a sensitivity of 91% for identifying donor kidneys with acute tubular necrosis but ultimately good allograft function, as compared with allografts that ultimately displayed delayed graft function. In addition, in a preliminary study of renal allograft recipients, silver nanoparticle-enhanced spectra obtained from urine samples collected 1 day after surgery identified allografts at risk for future dysfunction.[28] The authors postulated free heme may be the source of the prognostic Raman peak in these samples.

As Raman spectroscopy is inexpensive and widely available in most academic environments, there exists considerable opportunity for its application to clinical diagnosis. Its exquisite molecular specificity, lack of sample preparation needs, and relatively simple instrumentation allow Raman spectroscopy to serve as a powerful adjunct to current histopathological techniques. Moreover, subtle variations in Raman spectra can be leveraged to recognize cell types and the tissue microenvironment, as well as to differentiate between various morphologically similar but biochemically distinct pathologies.[29,30] Raman has low sensitivity to water, and because handheld portable Raman spectrometers are commercially available, Raman spectroscopy is also well suited to the analysis of urine. Future work should explore the relationship between urine and kidney biopsy spectroscopy in crystalline nephropathies, with a possible goal of rendering a noninvasive diagnosis.

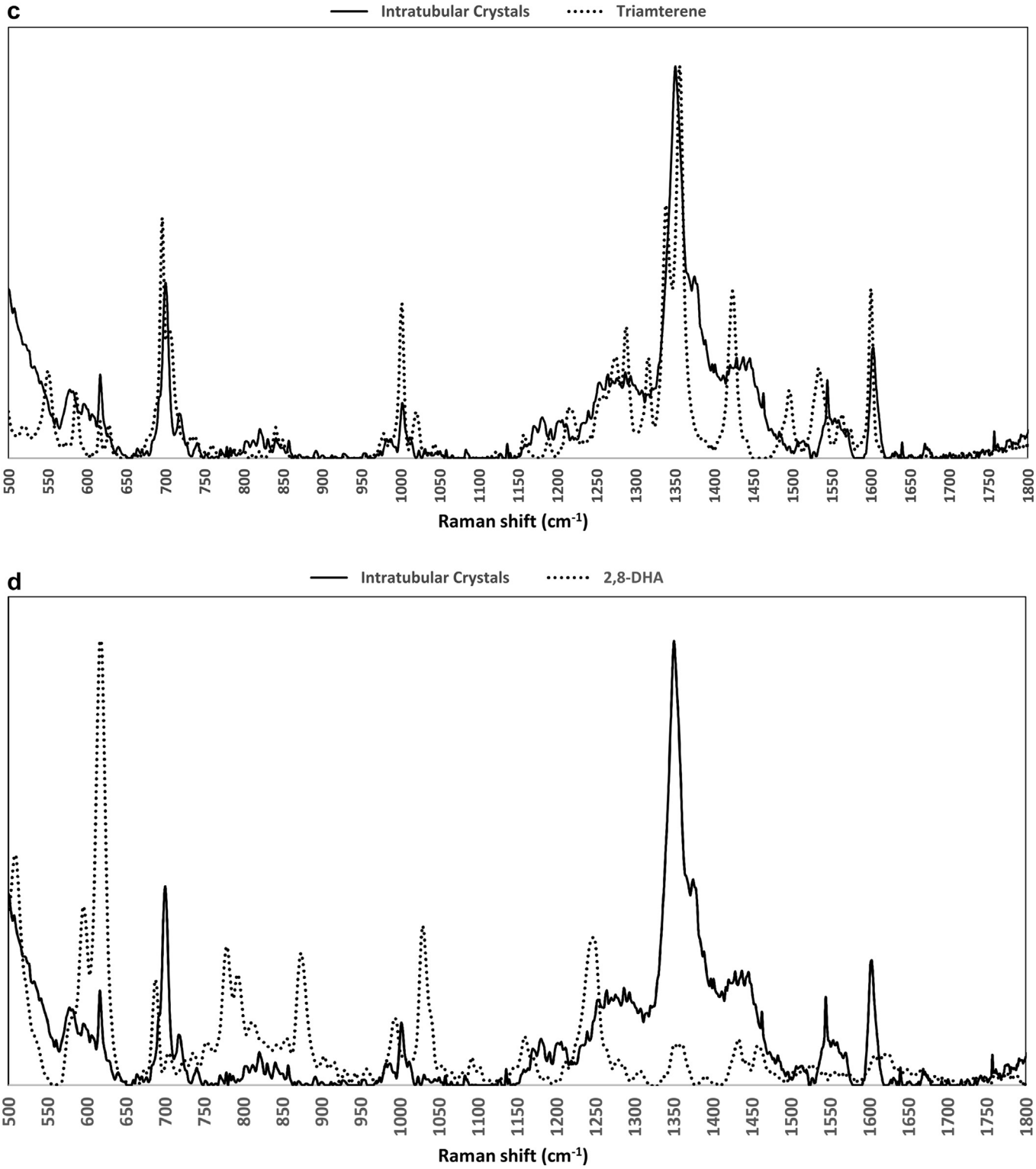

Figure 3. (Continued) (c) Overlay of Raman spectra of intratubular triamterene crystals (dotted) and prepared triamterene sample (solid). (d) Overlay of Raman spectra of intratubular triamterene crystals (dotted) and prepared 2,8-DHA sample (solid).

Table 2. Teaching points

Triamterene crystallization should be considered in the differential diagnosis of acute kidney injury.
Intratubular triamterene crystals are yellow-brown on hematoxylin-eosin and periodic acid-Schiff, black/gray on methenamine silver, pale blue on Masson trichrome stain, and under polarized light are birefringent with occasional Maltese cross formation.
Raman spectroscopy is a nondestructive, readily available imaging modality that can ascertain novel information from the kidney biopsy.

CONCLUSION

In summary, triamterene-associated crystalline nephropathy is a rare but potentially underrecognized clinical entity (Table 2). Clinicians should consider triamterene in the differential diagnosis of AKI and nephrolithiasis. Specific morphologic features can aid

in the identification of intratubular triamterene, but significant overlap can exist with 2,8-DHA and oxalate. The growing application of nontraditional technologies like Raman spectroscopy to the interpretation of kidney biopsy material highlights the value of extracting novel information from collected material.

DISCLOSURE

All the authors declared no competing interests.

AUTHOR CONTRIBUTIONS

CJS conceived the study, interpreted the data, drafted the manuscript, and provided intellectual content to the conduct of the work. CJS had full access to the data in the study and takes final responsibility for the decision to submit for publication. CZ performed Raman spectroscopy, interpreted the data, revised the manuscript, provided intellectual content to the conduct of the work, and approved the final draft. MD performed renal histology, revised the manuscript, provided intellectual content to the conduct of the work, and approved the final draft. RG performed renal histology, revised the manuscript, provided intellectual content to the conduct of the work, and approved the final draft. SB performed renal histology, revised the manuscript, provided intellectual content to the conduct of the work, and approved the final draft. IB performed Raman spectroscopy, interpreted the data, revised the manuscript, provided intellectual content to the conduct of the work, and approved the final draft.

REFERENCES

1. Fogazzi GB. Crystalluria: a neglected aspect of urinary sediment analysis. *Nephrol Dial Transplant*. 1996;11:379–387.
2. Yarlagadda SG, Perazella MA. Drug-induced crystal nephropathy: an update. *Expert Opin Drug Saf*. 2008;7:147–158.
3. Drug Usage Statistics, United States, 2004–2014. Hydrochlorothiazide; triamterene. Available at: http://clincalc.com/DrugStats/Drugs/HydrochlorothiazideTriamterene. Accessed October 7, 2017.
4. Varma VK, Kajdacsy-Balla A, Akkina SK, et al. A label-free approach by infrared spectroscopic imaging for interrogating the biochemistry of diabetic nephropathy progression. *Kidney Int*. 2016;89:1153–1159.
5. Krafft C, Popp J. The many facets of Raman spectroscopy for biomedical analysis. *Anal Bioanal Chem*. 2015;407:699–717.
6. Winnard PT Jr, Zhang C, Vesuna F, et al. Organ-specific isogenic metastatic breast cancer cell lines exhibit distinct Raman spectral signatures and metabolomes. *Oncotarget*. 2017;8:20266–20287.
7. Fairley KF, Birch DF, Haines I. Abnormal urinary sediment in patients on triamterene. *Lancet*. 1983;1:421–422.
8. Fairley KF, Woo KT, Birch DF, et al. Triamterene-induced crystalluria and cylinduria: clinical and experimental studies. *Clin Nephrol*. 1986;26:169–173.
9. Ettinger B, Weil E, Mandel NS, et al. Triamterene-induced nephrolithiasis. *Ann Intern Med*. 1979;91:745–746.
10. Daudon M, Jungers P. Drug-induced renal calculi: epidemiology, prevention and management. *Drugs*. 2004;64:245–275.
11. Farge D, Turner MW, Roy DR, et al. Dyazide-induced reversible acute renal failure associated with intracellular crystal deposition. *Am J Kidney Dis*. 1986;8:445–449.
12. Roy LF, Villeneuve JP, Dumont A, et al. Irreversible renal failure associated with triamterene. *Am J Nephrol*. 1991;11:486–488.
13. Nasr SH, Milliner DS, Wooldridge TD, et al. Triamterene crystalline nephropathy. *Am J Kidney Dis*. 2014;63:148–152.
14. Bollee G, Harambat J, Bensman A, et al. Adenine phosphoribosyltransferase deficiency. *Clin J Am Soc Nephrol*. 2012;7:1521–1527.
15. Zaidan M, Palsson R, Merieau E, et al. Recurrent 2,8-dihydroxyadenine nephropathy: a rare but preventable cause of renal allograft failure. *Am J Transplant*. 2014;14:2623–2632.
16. Runolfsdottir HL, Palsson R, Agustsdottir IM, et al. Kidney disease in adenine phosphoribosyltransferase deficiency. *Am J Kidney Dis*. 2016;67:431–438.
17. Daudon M, Protat MF, Reveillaud RJ, et al. Infrared spectrometry and Raman microprobe in the analysis of urinary calculi. *Kidney Int*. 1983;23:842–850.
18. Guerra-Lopez JR, Guida JA, Della Vedova CO. Infrared and Raman studies on renal stones: the use of second derivative infrared spectra. *Urol Res*. 2010;38:383–390.
19. Tonannavar J, Deshpande G, Yenagi J, et al. Identification of mineral compositions in some renal calculi by FT Raman and IR spectral analysis. *Spectrochim Acta A Mol Biomol Spectrosc*. 2016;154:20–26.
20. Pestaner JP, Mullick FG, Johnson FB, et al. Calcium oxalate crystals in human pathology. Molecular analysis with the laser Raman microprobe. *Arch Pathol Lab Med*. 1996;120:537–540.
21. Kummeling MT, de Jong BW, Laffeber C, et al. Tubular and interstitial nephrocalcinosis. *J Urol*. 2007;178:1097–1103.
22. Bazin D, Jouanneau C, Bertazzo S, et al. Combining field effect scanning electron microscopy, deep UV fluorescence, Raman, classical and synchrotron radiation Fourier transform infra-red spectroscopy in the study of crystal-containing kidney biopsies. *C R Chim*. 2016;19:1439–1450.
23. Dessombz A, Bazin D, Dumas P, et al. Shedding light on the chemical diversity of ectopic calcifications in kidney tissues: diagnostic and research aspects. *PLoS One*. 2011;6:e28007.
24. Vuiblet V, Nguyen TT, Wynckel A, et al. Contribution of Raman spectroscopy in nephrology: a candidate technique to detect hydroxyethyl starch of third generation in osmotic renal lesions. *Analyst*. 2015;140:7382–7390.
25. Vuiblet V, Fere M, Bankole E, et al. Raman-based detection of hydroxyethyl starch in kidney allograft biopsies as a potential marker of allograft quality in kidney transplant recipients. *Sci Rep*. 2016;6:33045.
26. Li J, Du Y, Qi J, et al. Raman spectroscopy as a diagnostic tool for monitoring acute nephritis. *J Biophotonics*. 2016;9:260–269.

27. Chi J, Ma Y, Weng FL, et al. Surface-enhanced Raman scattering analysis of urine from deceased donors as a prognostic tool for kidney transplant outcome. *J Biophotonics*. 2017;10:1743–1755.

28. Chi J, Zaw T, Cardona I, et al. Use of surface-enhanced Raman scattering as a prognostic indicator of acute kidney transplant rejection. *Biomed Opt Express*. 2015;6:761–769.

29. Paidi SK, Rizwan A, Zheng C, et al. Label-free Raman spectroscopy detects stromal adaptations in premetastatic lungs primed by breast cancer. *Cancer Res*. 2017;77:247–256.

30. Zhang C, Winnard PT, Dasari S, et al. Label-free Raman spectroscopy provides early determination and precise localization of breast cancer-colonized bone alterations. *Chem Sci*. 2018;9:743–753.